N72-12141 (NASA-CR-124672) A FAST ALGORITHM FOR THE CALCULATION OF JUNCTION CAPACITANCE AND ITS APPLICATION FOR IMPURITY PROFILE DETERMINATION H.J.J. DeMan (California Univ.) 1971 41 p CSCL 09C G3/09 Unclas 90016
(NASA CR OR TMX OR AD NUMBER) (CATEGORY)

A FAST ALGORITHM FOR THE CALCULATION OF JUNCTION CAPACITANCE AND ITS APPLICATION FOR IMPURITY PROFILE DETERMINATION

Hugo J. J. De Man*

Department of Electrical Engineering
University of California, Berkeley
Berkeley, California 94720

NASA Spon. P20

*On leave from the Catholic University of Louvain (Belgium)

Abstract.

A fast algorithm is described which calculates the space charge layer width and junction capacitance for an arbitrary impurity profile and for plane, cylindrical and spherical junctions.

The algorithm is based on the abrupt space charge edge (ASCE) approximation.

A method to use the algorithm for the determination of impurity profiles for two-sided junctions is presented. An expression is derived for the built-in voltage to be used for capacitance calculations with the ASCE approximation. Experimental evidence is given that the algorithm permits very accurate capacitance calculations and also predicts the exact temperature dependence of the junction capacitance.

List of symbols

A	:	mesa-diode area (cm^{-2})
α	:	profile parameter satisfying: $N_A = N_o \, erfc(\alpha)$
C	:	Junction capacitance (F)
C_k	:	k^{th} calculated capacitance value (F)
C_{mk}	:	k^{th} measured capacitance value (F)
D	:	diffusion coefficient of a dopant (cm^2/sec)
ε	:	permittivity of the semiconductor (F/cm)
$\mathcal{E}$	:	electric field in the depletion layer (V/cm)
k	:	Boltzmann constant
L	:	$L = 2\sqrt{Dt}$: characteristic diffusion length (cm)
$N(x)$	:	net impurity profile (cm^{-3})
n_i	:	intrinsic density of the semiconductor (cm^{-3})
N_A	:	substrate doping (cm^{-3})
N_o	:	surface concentration of diffusion dopant (cm^{-3})
$\vec{p}$	:	parameter vector in the profile function $N(x,p)$
q	:	electronic charge ($1.6 \; 10^{-19} C$)
t	:	diffusion time (sec)
V	:	electrostatic potential in the semiconductor
V_a	:	voltage applied to the diode (reverse bias is positive) (Volt)
V_b	:	built-in voltage used to calculate the depletion layer width. (Volt)

$V_{bt}(V_a) = (kT/q)\ \ln(|N(x_l(V_a)) \cdot N(x_r(V_a))| / n_i^2$: theoretical built-in voltage at voltage V_a

V_g : gradient voltage defined as the intercept of the tangent to a $C^{-3}(V_a)$ curve for $V_a = 0$

V_i : intercept with the V_a-axis of the $C^{-3}(V_a)$ curve (Volt)

x : coordinate axis in the semiconductor

$x_j(r_j)$: junction depth from the surface of the semiconductor

x_l : left-hand edge of the space charge layer

x_r : right-hand edge of the space charge layer

$\xi(\overline{p})$: performance index to calculate the profile parameters

I. Introduction.

Several authors have calculated the junction capacitance versus bias for some specific types of impurity profiles.[1,2,3,4] The results are usually represented by a normalized graph. These graphs are useful if only a few calculations are required and if the impurity profile corresponds to the one used to construct the graph. In many cases the profile is different and the junction capacitance or depletion layer width has to be used as part of a computer program for calculations of device behavior. In these cases it is convenient to have an efficient algorithm that calculates the depletion layer characteristics for any voltage, impurity profile and semiconductor material. Examples are: detailed modeling of JFET's, design of varactors [5], avalanche breakdown calculations [6], transistor modeling.[7]

Such an algorithm based on the abrupt space charge edge (ASCE) approximation [4] and an application of it to the determination of impurity profiles for two-sided junctions is described here.

It is recognized that more elaborate programs exist [8,9] that calculate the exact capacitance taking the mobile charge carriers into account. However, it has been shown [9,10] that, for capacitance calculations, a simple correction to the theoretical built-in voltage at zero bias, ($V_{bt}(0)$), can account for the mobile carriers. A more general expression for this correction is derived here. It is valid at any temperature and for any semiconductor. As a result the ASCE approximation can be used for capacitance calculations, thus saving a considerable amount of computer time. Moreover, even in the exact programs computation time is saved if the Gummel's Iteration method [8] is started from a first guess calculated from the ASCE approximation. This is another application for the algorithm presented here.

II. The algorithm.

The algorithm consists of two parts: the starting algorithm and the Newton's iteration. The latter is described first.

a. Newton's iteration.

Let N(x) represent an impurity profile function such that:

$$N(x) > 0 \quad \text{for} \quad x < 0 \tag{1a}$$

$$N(x) < 0 \quad \text{for} \quad x > 0 \tag{1b}$$

The function N(x) need not to be continuous at x = 0 which is the location of the metallurgical junction (fig. 1). The conditions (1a,b) are no limitations since any profile can satisfy (1a,b) by a change in bias polarity and the sign of $N(x)$. x_1 and x_r are the abrupt space charge edges. Let us assume, for the time being, that the built-in voltage V_b is known. It is easy to show that the double integration of Poisson's equation:

$$\frac{d^2V}{dx^2} = -\frac{qN(x)}{\varepsilon} \tag{2}$$

with boundary conditions:

$$\left.\frac{dV}{dx}\right|_{x=x_1} = 0 \tag{3}$$

$$\left.\frac{dV}{dx}\right|_{x=x_r} = 0 \tag{4}$$

yields:

$$F(x_r, x_1) \triangleq \int_{x_1}^{x_r} N(x)dx = 0 \tag{5}$$

$$G(x_r, x_1) \triangleq \int_{x_1}^{x_r} xN(x)dx + \frac{\varepsilon}{q}(V_a + V_b) = 0 \tag{6}$$

Note that V_a is considered to be positive for reverse bias and that (3) and (4) are approximations stating that the electric field vanishes at the space charge edges. It has been shown [10] that this approximation can also be corrected by using the appropriate V_b. Equations (5) and (6) are the basic set of equations for x_1 and x_r. Equations (5) and (6) can be solved numerically with Newton's iteration method. Once x_r and x_l are known the capacitance is given by:

$$C = \frac{\varepsilon A}{x_r - x_l} \tag{7}$$

Let $(x_r^{(i)}, x_l^{(i)})$ be the result of the i^{th} iteration and let

$$x_r^{(i+1)} = x_r^{(i)} + \Delta x_r^{(i)} \tag{8}$$

$$x_l^{(i+1)} = x_l^{(i)} + \Delta x_l^{(i)} \tag{9}$$

be a better approximation. Let further $F^{(i)} = F(x_r^{(i)}, x_l^{(i)})$ and $G^{(i)} = G(x_r^{(i)}, x_l^{(i)})$. Accordingly,

$$\begin{vmatrix} \frac{\partial F^{(i)}}{\partial x_r} & \frac{\partial F^{(i)}}{\partial x_l} \\ \frac{\partial G^{(i)}}{\partial x_r} & \frac{\partial G^{(i)}}{\partial x_l} \end{vmatrix} \cdot \begin{vmatrix} \Delta x_r^{(i)} \\ \Delta x_l^{(i)} \end{vmatrix} = - \begin{vmatrix} F^{(i)} \\ G^{(i)} \end{vmatrix} \tag{10}$$

Carrying out the differentiations on (5) and (6) we have:

$$\begin{vmatrix} N(x_r^{(i)}) & -N(x_l^{(i)}) \\ x_r^{(i)} N(x_r^{(i)}) & -x_l^{(i)} N(x_l^{(i)}) \end{vmatrix} \cdot \begin{vmatrix} \Delta x_r^{(i)} \\ \Delta x_l^{(i)} \end{vmatrix} = - \begin{vmatrix} F^{(i)} \\ G^{(i)} \end{vmatrix} \tag{11}$$

Equation (11) shows the advantage of applying Newton's method since the calculation of the partial derivatives $\partial F/\partial x_{r,l}$ and

$\partial G/\partial x_{r,1}$ requires only two profile function calculations. Apparently the calculation of the right hand side of (11) requires two accurate numerical integrations for each iteration. However, with $(x_r^{(1)}, x_1^{(1)})$ representing the starting values for the iteration, $F^{(i)}$ can be written as:

$$F^{(i)} = \int_{x_1^{(i)}}^{x_r^{(i)}} N(x)dx = \int_{x_1^{(1)}}^{x_r^{(1)}} N(x)dx + \sum_{k=1}^{i-1} \int_{x_r^{(k)}}^{x_r^{(k+1)}} N(x)dx + \sum_{k=1}^{i-1} \int_{x_1^{(k+1)}}^{x_1^{(k)}} N(x)dx \tag{12}$$

If $(x_r^{(1)}, x_1^{(1)})$ is close enough to the solution, then at each iteration the intervals $(x_r^{(k)}, x_r^{(k+1)})$ and $(x_1^{(k+1)}, x_1^{(k)})$ are small enough to use a three point Simpson iteration such that at the i^{th} iteration we only calculate for example:

$$\int_{x_r^{(i)}}^{x_r^{(i+1)}} N(x)dx \approx \frac{x_r^{(i)}}{3}\left[N(x_r^{(i)}) + 4N((x_r^{(i)} + x_r^{(i+1)})/2)) + N(x_r^{(i+1)})\right] \tag{13}$$

Since $N(x_r^{(i)})$ is known from the previous step it is easy to show that for each Newton iteration, except for the first, only four new function evaluations need to be done to update $F^{(i)}$ and $G^{(i)}$ and to calculate the next iteration point. Usually three iterations are sufficient for a relative accuracy of 10^{-5} for (x_r, x_1), such that about twelve function evaluations are needed in this part of the algorithm. The problem is now to find appropriate starting values $(x_r^{(1)}, x_1^{(1)})$.

b. The starting algorithm.

A method for the calculation of $(x_r^{(1)}, x_l^{(1)})$ that permits the calculation of $F^{(1)}$ and $G^{(1)}$ at almost no extra cost will be described.

Let x_{rm} and x_{lm} be defined from:

$$G(x_{rm},0) \triangleq \int_0^{x_{rm}} xN(x)dx + \frac{\varepsilon}{q}(V_a + V_b) \equiv 0 \qquad (14)$$

$$G(0,x_{lm}) \triangleq \int_{x_{lm}}^{0} xN(x)dx + \frac{\varepsilon}{q}(V_a + V_b) \equiv 0 \qquad (15)$$

Then from (1a,b) and (5) and (6) it follows that:

$$x_{rm} = \sup (x_r) \quad \text{and} \quad x_{lm} = \inf (x_l)$$

Further $G(x_r,x_l)$ defines a curve $x_l = g(x_r)$ in the (x_r,x_l) plane (fig. 2) going through $A(0,x_{lm})$ and $B(x_{rm},0)$ and having a derivative:

$$g'(x_r) = \frac{dx_l}{dx_r} = - \frac{\partial G/\partial x_r}{\partial G/\partial x_l} = \frac{x_r N(x_r)}{x_l N(x_l)} > 0 \qquad (16)$$

as can be found from conditions (1a,b). Further from (16):

$$g'(0) = 0 \qquad (17)$$

and $$g'(x_{rm}) = +\infty \qquad (18)$$

From (16), (17) and (18) it follows that $x_l = g(x_r)$ is a curve of the form indicated in fig. 2 by curve 1.

The function $F(x_r,x_l)$ defines a curve $x_l = f(x_r)$ in the (x_r,x_l) plane, going through the origin 0 (fig. 2) and having a derivative:

$$f'(x_r) = -\frac{\partial F/\partial x_r}{\partial F/\partial x_l} = \frac{N(x_r)}{N(x_l)} < 0 \tag{19}$$

by condition (1a,b). It is a decreasing function represented by curve 2 on fig. 2.

The intersection $C(x_r, x_l)$ is the solution to the problem. The point $D(x_r^{(1)}, x_l^{(1)})$ is considered as the starting value for Newton's method. This point is obtained as follows:

a. For a given $N(x)$, V_a and V_b, find x_{rm} and x_{lm} (points A and B in fig. 2)

b. Find the intersection I of the line AB and $x_l = f(x_r)$

c. Calculate the intersection, D, with the curve $x_l = g(x_r)$ of the tangent line t to $x_l = f(x_r)$ in point I.

Note that the equation for t is simply given by:

$$(x_l - x_{li}) = -\frac{N(x_{ri})}{N(x_{li})}(x_r - x_{ri}) \tag{20}$$

In all practical cases, point D is within 10% of the required solution. Note also that since D is only a starting point, it does not need to be calculated with high precision. Details of the starting algorithm are given in Appendix A. Basically the method consists of a stepping along the x_l and x_r axis to find approximations for x_{rm} and x_{lm}. During this operation a maximum of 50 but typically 40 function values are calculated only once and stored in the memory. These values are then used in arithmetic operations only to find I and D. At the same time these stored values are used in Simpson's rule to calculate $F^{(1)}$ and $G^{(1)}$. The total number of function evaluations to find (x_r, x_l) is typically 60-65 for three Newton iterations.

It should be noted that:

a. The above described algorithm can easily be adapted to calculate both cylindrical and spherical junctions as indicated in appendix B.

b. If (x_r, x_l) has to be calculated for many successive voltages V_a, the starting algorithm is used only once. The preceding values of (x_r, x_l) are then used as starting values for the next voltage.

III. The built-in voltage V_b.

Depending on the use of the algorithm we consider three possibilities for V_b.

a. A known V_b.

This is the case, for example, if the algorithm is used to calculate impurity profiles from $C(V_a)$ measurements as described in section IVa. This case is trivial since the basic algorithm can be used without modification.

b. <u>The algorithm is used to calculate approximate field and potential distributions</u>.

In this case V_b is given by:

$$V_b = V_{bt}(V_a) = \frac{kT}{q} \ln \left| \frac{N(x_r(V_a))\ N(x_l(V_a))}{n_i^2} \right| = V_b(x_r, x_l) \quad (21)$$

Strictly speaking, the method of section II becomes invalid since V_b is itself a function of the solution (x_r, x_l). Due to the logarithmic dependence, $V_b(x_r, x_l)$ is a slowly varying function and thus the following procedure can be used. The algorithm is started with $V_b^{(0)} = 0.7$ Volt as a first guess. From the starting algorithm $(x_r^{(1)}, x_l^{(1)})$ are found and $V_b^{(1)} = V_b(x_r^{(1)}, x_l^{(1)})$ can be calculated and used in Newton's iteration. This gives a first approximation (x_{r1}, x_{l1}) for the solution (x_r, x_l). $V_b^{(2)} = V_b(x_{r1}, x_{l1})$ is then a better approximation for V_b and with $V_b^{(2)}$ and (x_{r1}, x_{l1}) as new starting values Newton's iteration is used again. This is repeated until:

$$\left| V_b^{(i+1)} - V_b^{(i)} \right| \leq 0.1 \text{ mV}$$

which occurs after 2 ... 3 Newton iteration cycles.

If necessary the field - and potential distributions can be found from:

$$\mathcal{E}(x) = -\frac{dV}{dx} = -\frac{q}{\varepsilon}\int_{x_1}^{x} N(\xi)\,d\xi \qquad (22)$$

$$V(x) - V(x_1) = -\frac{q}{\varepsilon}\left[x\,\mathcal{E}(x) + \int_{x_1}^{x} \xi N(\xi)\,d\xi\right] \qquad (23)$$

Equations (22) and (23) follow from the integration of (2), using (3). The numerical integration of (22) and (23) can be done using the function values stored during the starting algorithm, such that $\mathcal{E}(x)$ and $V(x)$ are found without too many extra calculations. This is useful for breakdown and avalanche multiplication calculations.

c. <u>Capacitance calculations</u>.

Almost all diffused junctions (and even epitaxial junctions) behave almost as linear junctions at low reverse and forward bias [4, 6] i.e. $C^{-3}(V_a)$ is indistinguishible from a linear function intersecting the V_a axis at the intercept voltage V_i. Nuyts and Van Overstraeten [9,10] have shown numerically that almost correct junction capacitances can be calculated with the ASCE approximation if the built-in voltage V_b is taken equal to the intercept voltage V_i given by:

$$V_i = V_{bt}(0) - V_{bc} \qquad (24)$$

They found $V_{bc} \approx 0.13$ Volt for silicon, at room temperature. Using the concept of "gradient" voltage, introduced by Chawla and Gummel[4] it is possible to find a more general expression for V_{bc}. The gradient voltage V_g is the intercept voltage of a tangent to the $C^{-3}(V_a)$ curve for $V_a = 0$ volt and is shown[4] to be:

$$V_g = \frac{2}{3}\frac{kT}{q} \ln \frac{a^2 \varepsilon kT}{8q^2 n_i^3} \qquad (25)$$

Nuyts[10] has shown that the gradient voltage is 2kT/3 higher than the intercept voltage V_i used in (24). As a result:

$$V_i = V_{bt}(0) - V_{bc} = \frac{2}{3}\frac{kT}{q}\left[\ln \frac{a^2 \varepsilon kT}{8q^2 n_i^3} - 1\right] \qquad (26)$$

We also have:

$$V_{bt}(0) = \frac{kT}{q} \ln \frac{a^2\ w^2(0)}{n_i^2} \qquad (27)$$

and $$w(0) = \left(\frac{12\varepsilon V_{bt}(0)}{qa}\right)^{1/3} \qquad (28)$$

After elimination of w(0) and a from (26), (27) and (28) and solving for V_{bc}:

$$V_{bc} = \frac{2}{3}\frac{kT}{q}\left[\ln\left(\frac{12qV_{bt}(0)}{kT}\right) + 1\right] \qquad (29)$$

Such that:

$$V_b = V_{bt}(0) - \frac{2}{3}\frac{kT}{q}\left[\ln\left(\frac{12qV_{bt}(0)}{kT}\right) + 1\right] \qquad (30)$$

For silicon at room temperature and assuming $V_{bt}(0) = 0.8079$ Volt for $a = 10^{22}\ cm^{-4}$ [4], (29) gives $V_{bc} = 0.120$ Volt which is in good agreement with $V_b = 0.13$ Volt found by Nuyts and Van Overstraeten. The procedure for calculating $C(V_a)$ curves is now:

a. Set $V_a=0$ and calculate $V_{bt}(0)$ according to the method described in II b.

b. Calculate V_b from (30).

c. Since V_b is known now, calculate $C(V_a)$ for all given V_a using the basic algorithm.

IV. Applications.

a. Impurity profile determination for two-sided junctions.

The determination of a profile on a two-sided junction is only possible if the profile is exactly known on one side[11]. This is not the case for most diffused devices. Very often however it is possible to formulate an analytical expression describing the profile around the metallurgical junction. This expression depends on a parameter-vector $\overline{p}$ and can thus be written as:

$$N = N(x,\overline{p}) \qquad (31)$$

The vector $\overline{p}$ has to be found such that (31) gives the measured $C(V_a)$ dependence. In order to keep mathematics simple we describe the case for measurements on mesa-diodes although the method can easily be adapted to planar junctions using the expression for cylindrical and spherical junctions as given in Appendix B. The disadvantage is that for planar junctions the computer time is almost doubled by the additional calculations.

Let $C_{mk} = C_{mk}(V_{ak})$ be the measured capacitance values at the voltages V_{ak} where $k = 1, 2 \ldots m$ and m is the total number of capacitance measurements from slight forward bias (-0.5V) up to breakdown voltage. First the built-in voltage V_b is calculated. This is done by fitting a straight line through the points $C_{mk}^{-3}(V_{ak})$ for $-0.5 \leqslant V_{ak} \leqslant 0.1$ Volt. The intercept V_i of this line with the V_a-axis is the built-in voltage V_b. Once V_b known we can calculate, for a given $N(x, \bar{p})$:

$$C_k = C_k(V_{ak}, V_b, \bar{p}) = \frac{\varepsilon A}{x_{rk}(\bar{p}) - x_{1k}(\bar{p})} \tag{32}$$

$x_{rk}(\bar{p})$ and $x_{1k}(\bar{p})$ are calculated from the basic algorithm for the given $N(x, \bar{p})$, V_{ak} and V_b.

We now define a performance index:

$$\xi(\bar{p}) \triangleq \sum_{k=1}^{m} \left[\frac{C_k - C_{mk}}{C_{mk}}\right]^2 \tag{33}$$

If $\bar{p}_m$ is found such that:

$$\xi(\bar{p}_m) = \underset{\forall \bar{p}}{\mathrm{Min}}\; \xi(\bar{p}) \tag{34}$$

Then the impurity profile corresponding to the $C(V_a)$ measurements is given by:

$$N(x) = N(x, \overline{p}_m) \tag{35}$$

Efficient algorithms to minimize $\xi(\overline{p})$ such as Fletcher-Powell's[12] method require the evaluation of the gradient $\overline{g} = \partial\xi / \partial \overline{p}$. Perturbation methods to calculate $\overline{g}$ are very inefficient in time and are too inaccurate. A more efficient way starts from the definition (33) of $\xi(\overline{p})$:

$$g_j = \frac{\partial \xi(\overline{p})}{\partial p_j} = 2\sum_{k=1}^{m} \frac{(C_k - C_{mk})}{C_{mk}^2} \frac{\partial C_k(\overline{p})}{\partial p_j} \tag{36}$$

From (36) and (32):

$$g_j = -\frac{2}{\varepsilon \cdot A} \sum_{k=1}^{m} \frac{C_k^2}{C_{mk}^2} (C_k - C_{mk}) \left(\frac{\partial x_r}{\partial p_j} - \frac{\partial x_l}{\partial p_j} \right) \tag{37}$$

The problem is reduced now to the calculation of $\partial x_r / \partial p_j$ and $\partial x_l / \partial p_j$. Therefore consider eq.(5) and (6) where $N(x)$ is substituted by $N(x, \overline{p})$ such that $F(x_r, x_l)$ and $G(x_r, x_l)$ become $F(x_r, x_l, \overline{p})$ and $G(x_r, x_l, \overline{p})$. Taking the total differential of F and G with respect to x_r, x_l and p_j yields:

$$\begin{vmatrix} x_r N(x_r,\overline{p}) & -x_l N(x_l,\overline{p}) \\ N(x_r,\overline{p}) & -N(x_l,\overline{p}) \end{vmatrix} \cdot \begin{vmatrix} \dfrac{\partial x_r}{\partial p_j} \\ \dfrac{\partial x_l}{\partial p_j} \end{vmatrix} = - \begin{vmatrix} \displaystyle\int_{x_l}^{x_r} x \frac{\partial N(x,\overline{p})}{\partial p_j} dx \\ \displaystyle\int_{x_l}^{x_r} \frac{\partial N(x,\overline{p})}{\partial p_j} dx \end{vmatrix} \tag{38}$$

A comparison of (38) with (11) indicates that the left-handside-matrix is already calculated during the last Newton iteration in the basic algorithm. Calculating a gradient component thus requires for each voltage only the calculation of the two integrals in the right-handside of (38). If succesive increasing voltage steps are used, former calculated values can be used and a simple integration rule can be applied in the same way as described in IIa for the calculation of $F^{(i)}$ and $G^{(i)}$ (eq. (12) and (13)).

As an example a phosphorus diffusion from a $POCl_3$ source at 1075°C for 30 min. in a uniformly doped p substrate of 0.2 Ωcm is considered. It is known [13, 14] that the ionized impurity profile can be described as almost constant and equal to about $N_o = 2.5\ 10^{20}\ cm^{-3}$ from the surface to some depth x_l (fig. 2). From there up to the junction depth x_j the profile behaves almost as a complementary errorfunction.

In order to be consistent with the definition (1a,b) of $N(x)$ we take the origin at the junction. It is easy to show that the profile around the junction can be written as:

$$N(x) = -\frac{2N_o}{\sqrt{\pi}} \int_{\alpha}^{\frac{x}{L}+\alpha} e^{-\xi^2}\, d\xi = N(x,L,\alpha) \qquad (39)$$

where $N_o = 2.5\ 10^{20}\ \text{cm}^{-3}$, $L = 2\sqrt{Dt}$ and α is such that the substrate doping N_A is given by:

$$N_A = N_o\ \text{erfc}\ (\alpha) \qquad (40)$$

Since N_o is assumed to be known, the parameter vector $\overline{p}$ is given by:

$$\overline{p} = (L,\alpha)$$

A mesa diode of an area $A = 10^{-3}\text{cm}^{-3}$ was made from the diffused wafer and the $C(V_a)$ curve was measured with a Boonton 75A bridge. The measured points are given in column I and II of table 1. Curve 4 on fig. 4 gives $C^{-3}(V_a)$ for forward bias. From this figure the intercept voltage V_i is read to be:

$$V_i = V_b = 0.680\ \text{V}$$

Using this value for V_b and taking $\varepsilon = 1.04\ 10^{-12}$ F/cm for silicon the above described curve fitting technique, with a Fletcher-Powell minimization routine, was performed for the 17 $C(V_a)$ points. Starting values for $\overline{p}$ are:

$\alpha = 2.3$

and $L = 4.10^{-5}$ cm.

The $C(V_a)$ values calculated from these starting values are given in column III of table 1. The mean error is about 40%. After 6 iterations, requiring 10 sec. CPU time on the CDC 6400 computer, convergence was obtained for the following parameters:

$\alpha = 2.438$

$L = 5.742 \; 10^{-5}$ cm

$x_2 = 1.40 \; \mu m$

$N_A = 1.413 \; 10^{17} cm^{-3}$

The mean error for these final values is 0.3% which is within the experimental error of the $C(V_a)$ measurements indicating that the erfc, is a good approximation to the profile. The capacitance calculated from the final profile parameter are given in column III of table 1. Note the very close agreement with the measured values. The diffusion depth was measured to be $x_j = 2.27 \mu m$ such that the profile can be constructed as is done in fig. 3. The sheet-resistivity calculated from this profile using Irvin's[15] method gives $\rho_s = 2.92 \Omega/\square$, which is in good agreement with the measured value of $2.8 \Omega/\square$. Note also that the computed result $N_A = 1.413 \; 10^{17} cm^{-3}$ is close to $N_A = 1.5 \ldots 2.0 \; 10^{17} cm^{-3}$ which is derived from the resistivity of the substrate. This example illustrates how the algorithm can be used to fit impurity profiles to $C(V_a)$ measurements.

b. Calculation of $C(V_a)$ curves.

Using the above-determined profile parameters, we can calculate $C(V_a)$ curves at different temperatures using the procedure described in section IIc. and compare the results with measurements. Fig. 4 is a set of measured $C^{-3}(V_a)$ curves at six different temperatures. The intercepts with the V_a-axis of the straight lines through the experimental points represent the measured built-in voltage at the different temperatures. The crosses are calculated points and the crosses on the V_a axis represent the V_b values calculated from (30).

Fig. 5 shows calculated C(T) curves at different bias points using V_b given by eq. (30). The dots are again measured values. Note the large temperature sensitivity for forward bias due to the important role of $V_b(T)$. It is obvious from fig. 4 and 5. that the use of eq. (30) for V_b makes accurate capacitance calculations possible with the ASCE approximation, even for moderate forward bias levels. Moreover eq. (30) also describes the temperature dependence of V_b accurately. This is illustrated in fig. 6 where the built-in voltage calculated from (30) is plotted and compared with measured values indicated by the dots. The agreement is quite well over the temperature range considered here. Note that $\Delta V_b/\Delta T \approx -2mV/^{o}C$ for the (-55, 125^{o}C) temperature range. This value is fairly typical for most junctions in I.C. transistors.

V. Conclusion.

A fast algorithm has been described which calculates the junction capacitance for an arbitrary impurity profile and applied voltage V_a. It is shown that due to the form of the basic equations, Newton's method is especially efficient to use. The algorithm is based on the abrupt space charge edge (ASCE) approximation. It is found that, by an appropriate correction to the theoretical built-in voltage $V_{bt}(0)$, almost exact $C(V_a)$ curves can be calculated even for forward bias and at different temperatures.

On the other hand, it is shown how the algorithm can be used to calculate the parameters of an analytical expression for an impurity profile from a measured $C(V_a)$ curve.

I	II	III	IV
V_{ak} (Volts)	C_{mk} (pF)	C_k (final)(pF)	C_k (initial)(pF)
-0.4030	87.70	87.42	108.0
-0.3503	82.39	82.43	101.9
-0.3020	78.45	78.70	97.28
-0.2500	75.25	75.34	93.15
-0.1483	70.07	70.10	86.72
-0.5070	66.16	66.20	81.93
0.	64.52	64.47	79.82
0.2058	58.93	58.90	72.99
1.0000	47.27	47.24	58.73
3.038	35.64	35.74	44.70
4.015	32.80	32.87	41.22
6.008	29.07	28.91	36.41
8.067	26.27	26.18	33.10
10.01	24.39	24.29	30.81
12.11	22.68	22.69	28.88
13.15	21.97	22.02	28.07
14.82	20.98	21.07	26.93

Table 1.

Column I: Applied voltage V_{ak} (positive for reverse bias) (Volt)

Column II: Measured capacitance values (pF)

Column III: Calculated capacitance from the final profile parameters

Column IV: Calculated capacitance from the initial profile parameters

Acknowledgements

The author wishes to express his gratitude to the ESRO and NASA organizations for sponsoring this research, to the University of California, Berkeley I.C. laboratory and computer center for providing the facilities for this work and to Dr. M. Petrescu for many valuable discussions.

References

1. H. LAWRENCE and R.M. WARNER, Bell Syst. Techn. J. Vol 38, 389, (1960).

2. P.R. WILSON, Solid-St. Electron. Vol 12, 1, (1969).

3. P.R. WILSON, Solid-St. Electron. Vol 12, 277, (1969).

4. B.R. CHAWLA and H.K. GUMMEL, IEEE Trans on Electron Dev., Vol ED-18, 178, (1971).

5. H. YONEZU and A. KAWAJI, IEEE Trans on Electron Dev., Vol ED-16, 923, (1969).

6. R.J. VAN OVERSTRAETEN and H. DE MAN, Solid-St. Electron. Vol 13, 583, (1970).

7. R.E. THOMAS and A.R. BOOTHROYD, Solid-St. Electron. Vol 11, 365, (1968).

8. H.K. GUMMEL, IEEE Trans on Electron Dev., Vol ED-11, 455, (1964).

9. W. NUYTS and R.J. VAN OVERSTRAETEN, Electronics Letters, Vol 5, 54, (1969).

10. W. NUYTS, Ph. D. dissertation, Dept. of Electrical Engineering of the University of Louvain, Belgium.

11. H.J.J. De Man, IEEE Trans on Electron Dev. Vol ED-17, 1087, (1970).

12. R. FLETCHER and M.J.D. POWELL, Computer Journ. Vol 6, 163, (1963).

13. E. TANNENBAUM, Solid-St. Electron. Vol 2, 123, (1961).

14. R.A. McDONALD, G.G. EHLENBERGER, T.R. HUFFMAN, Vol 9, 807, (1966).

15. J.C. IRVIN, Bell Syst. Techn. Journ., Vol 41, 387, (1962).

Appendix A: The starting algorithm.

a. The search for x_{rm} and x_{lm}.

The search for x_{rm} will be described since the x_{lm} search is analoguous. A first rough guess for x_{rm} is made by calculating n such that:

$$\int_0^{\alpha} xN(x)dx + \sum_{k=1}^{n} \int_{\alpha.3^{k-1}}^{\alpha.3^{k}} xN(x)dx + \frac{\varepsilon}{q}(V_a+V_b) \leqslant 0 \qquad \text{(A1)}$$

α is choosen as 10^{-5} cm. A three-point Gaussian integration is used for calculating the integrals. The summation stops when (A1) is satisfied. From (A1) and (14) it follows:

$$\alpha.3^{n-1} \leqslant x_{rm} \leqslant \alpha.3^{n} \qquad \text{(A2)}$$

We now assume a stepsize Δ_r along the x_r-axis given by:

$$\Delta_r = 0.1\alpha 3^{n-1} \qquad \text{(A3)}$$

This is used in a trapezoidal integration to find a point $n_r\Delta_r$ such that:

$$\int_{T\,0}^{n_r\Delta_r} xN(x)dx + \frac{\varepsilon}{q}(V_a+V_b) \leqslant 0 \qquad \text{(A4)}$$

The symbol $\int_T$ indicates trapezoidal integration. Note that the search for n_r is done by a simple stepping along the x_r-axis until (A4) is satisfied. In the same way a step Δ_l is calculated on the x_1-axis and a point $-n_1\Delta_1$ is searched such that:

$$\int_{-n_1\Delta_1}^{0} xN(x)dx + \frac{\mathcal{E}}{q}(V_a + V_b) \leqslant 0 \tag{A5}$$

From (A4), (A5), (14) and (15) it follows that:

$$x_{rm} \approx n_r\Delta_r \tag{A6}$$

$$x_{lm} \approx -\hat{n}_l\Delta_l \tag{A7}$$

Note: 1. The exact values of x_{rm} and x_{lm} are not important, so (A6) and (A7) are considered correct.

2. During operations (A4) and (A5) all the function values $\varphi(\pm k)$ and partial integration results $S_x(\pm k)$ defined as:

$$\varphi(k) = N(k\Delta_r) \text{ and } S_x(k) = \int_{0}^{k\Delta_r} xN(x)dx \tag{A9}$$

$$\varphi(-k) = N(-k\Delta_r) \text{and } S_x(-k) = \int_{-k\Delta_l}^{0} xN(x)dx \tag{A10}$$

are stored. From (A2) and (A3) it follows that $n_{r,l} \leq 30$.

b. Search for $I(x_{li}, x_{ri})$ (fig. 2)

The equation of line AB (fig. 2) is:

$$x_l(x_r) = x_{lm}(1 - \frac{x_r}{x_{rm}}) \tag{A11}$$

Thus x_{ri} is the solution of:

$$\int_{x_l(x_{ri})}^{x_{ri}} N(x)dx = 0 \tag{A12}$$

This equation is solved with the trapezoidal integration by stepping along the x_r-axis with steps Δ_r. The trapezoidal integration makes use of the values $\varphi(\pm k)$ already stored so that no additional function values are calculated. A linear interpolation is used whenever the coordinates do not coincide with the grid defined by the steps Δ_r and Δ_l (this can be the case for $x_l(x_{ri})$). Note that from (A12) it follows:

$$\int_{x_{li}}^{x_{ri}} N(x)dx = 0 \tag{A13}$$

c. <u>Search for $(x_r^{(1)}, x_l^{(1)})$.</u>

The equation of the tangent line t (fig. 2) is:

$$x_l(x_r) = x_{li} - \frac{N(x_{ri})}{N(x_{li})}(x_r - x_{ri}) \tag{A14}$$

$x_r^{(1)}$ is the solution of:

$$\int_{x_l(x_r^{(1)})}^{x_r^{(1)}} xN(x)dx + \frac{\varepsilon}{q}(V_a+V_b) = 0 \tag{A15}$$

This equation is solved in the same way as in step b. . Use is made of the stored results $S_x(\pm k)$ and linear interpolations. Here too no new function calculations are required. Note that now, according to (A15):

$$G^{(1)} = G(x_1^{(1)}, x_r^{(1)}) = 0 \tag{A16}$$

so that $G^{(1)}$ is obtained at no extra cost. We only need to calculate:

$$F^{(1)} = F(x_1^{(1)}, x_r^{(1)})$$

which, according to A(13), is done by:

$$F^{(1)} = \int_{x_1^{(1)}}^{x_{1i}} {}_T N(x)dx + \int_{x_{ri}}^{x_r^{(1)}} {}_T N(x)dx \tag{A17}$$

making use of $\varphi(\pm k)$ values and linear interpolation. Note that function values are calculated only during the first step and then always used back again.

Appendix B: The cylindrical and spherical junction.

The cylindrical and spherical coordinates are defined in fig. 7. We assume that the profile function is given as:

$$N(x_{c,s}) = N(r - r_j) \tag{B1}$$

where the subscript c or s stands for cylindrical or spherical junctions respectively.

Poisson's equation can now be written as:

$$\frac{1}{r^n}\frac{d}{dr}\left(r^n \frac{dV}{dr}\right) = -\frac{qN(r-r_j)}{\varepsilon} \tag{B2}$$

with n=1 for cylindrical and n=2 for spherical junctions. It is easy to show that a double integration of (B2) and a change of coordinates to x_c or x_s leads to:

1. for cylindrical junctions:

$$F_c(x_{rc},x_{lc}) = \int_{x_{lc}}^{x_{rc}} \left(1 + \frac{x_c}{r_j}\right)N(x_c)dx_c = 0$$

$$G_c(x_{rc},x_{lc}) = r_j \int_{x_{lc}}^{x_{rc}} \left(1 + \frac{x_c}{r_j}\right)\ln\left(1 + \frac{x_c}{r_j}\right)N(x_c)dx_c + \frac{\varepsilon}{q}(V_a+V_b) = 0 \tag{B3}$$

2. for spherical junctions:

$$F_s(x_{rs}, x_{ls}) = \int_{x_{ls}}^{x_{rs}} (x_s + r_j)^2 N(x_s) dx_s = 0$$

$$G_s(x_{rs}, x_{ls}) = \int_{x_{ls}}^{x_{rs}} (x_s + r_j) N(x_s) dx + \frac{\mathcal{E}}{q}(V_a + V_b) = 0 \qquad \text{(B4)}$$

The equations (B3) or (B4) can be solved with Newton's method in exactly the same way as given in IIa. The partial derivatives in eq (10) are also easily calculated from only two function values and each iteration again requires only four function calculations. The starting values for (B3) are the solution (x_r, x_l) for the plane junction and for (B4) the solution (x_{rc}, x_{lc}) for the cylindrical junction. These are usually close enough to the solution if r_j is not too small. Moreover this is usually the sequence in which the results are needed (e.g. calculation for a rectangular planar diffusion such as collector-base or gate-drain junctions). The capacitance for one fourth of a cylindrical wall with length is then given as:

$$C_c = \frac{\pi \mathcal{E} 1}{2\ln\left(\frac{r_j - x_{lc}}{r_j + x_{rc}}\right)} \qquad \text{(B5)}$$

The capacitance for 1/8 sphere is given by:

$$C_s = \frac{\pi \varepsilon r_j (r_j - x_{ls})(r_j + x_{rs})}{4\,(x_{rs} - x_{ls})} \qquad \text{(B6)}$$

Captions to the figures.

Fig. 1 : Impurity profile definitions.

Fig. 2 : Representation of eq.(5) and (6) in the (x_r, x_l) plane. Curve 1 represents eq.(6) and curve 2 represents eq.(5). The intersection D of the tangent in point I to curve 2 is the starting point for the Newton iteration.

Fig. 3 : The impurity profile model for a phosphorus diffusion at $T > 1000^\circ C$ in a uniformly doped substrate with concentration N_A. The figure is drawn for the profile in the example i.e. $x_1 = 0.37 \mu m$; $x_2 = 1.40 \mu m$; $x_j = 2.27 \mu m$, $N_A = 1.413 \cdot 10^{17} cm^{-3}$ and $N_o = 2.5\ 10^{20} cm^{-3}$.

Fig. 4 : Measured (θ) and calculated (+) $C^{-3}(V_a)$ curves for forward bias and for six different temperatures. The intercepts V_i of the experimental curves at the different temperatures are given in the insert.

Fig. 5 : Calculated C(T) curves at different applied voltages V_a using V_L given by eq. (30). The dots represent measured points.

Fig. 6 : A comparison of $V_b(T)$ given by eq. (30) and experimental values (θ) for V_b.

Fig. 7 : Coordinate definitions for cylindrical and spherical junctions.

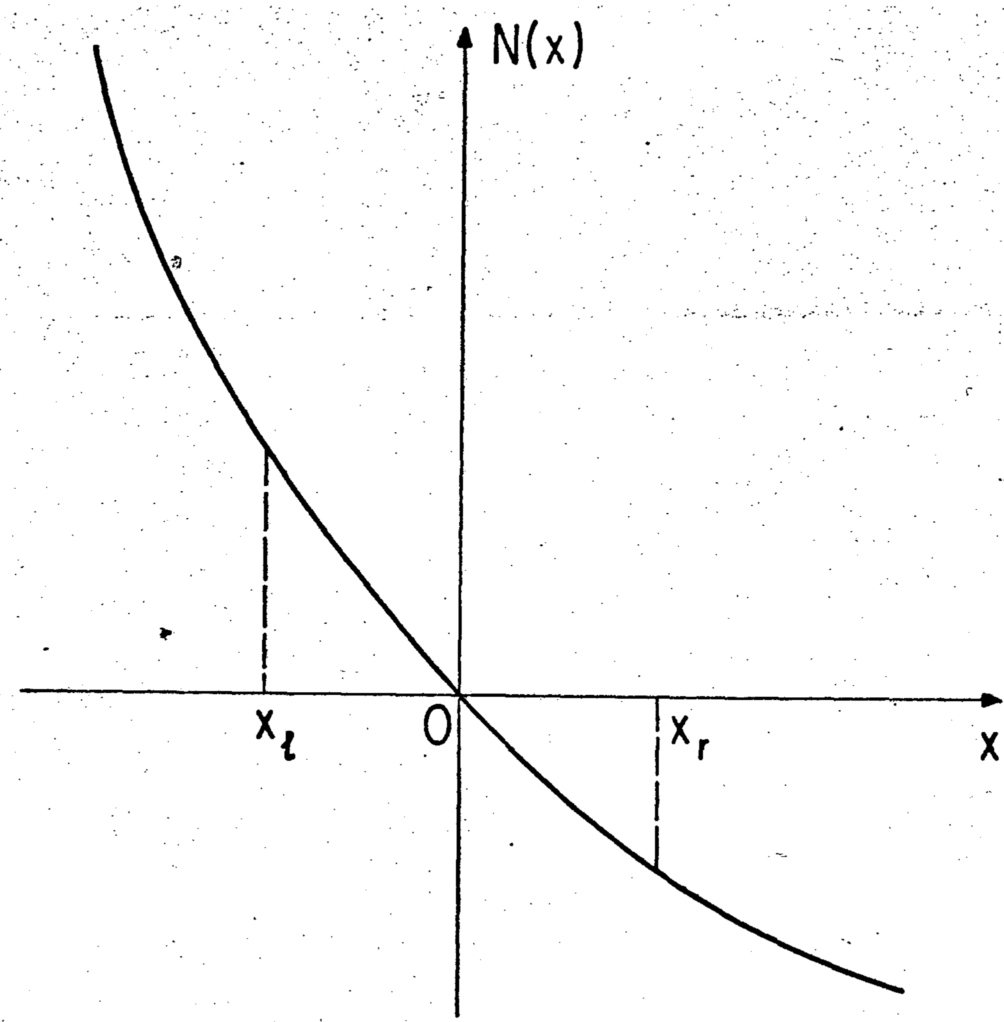

N(x)
x_ℓ
O
x_r
x

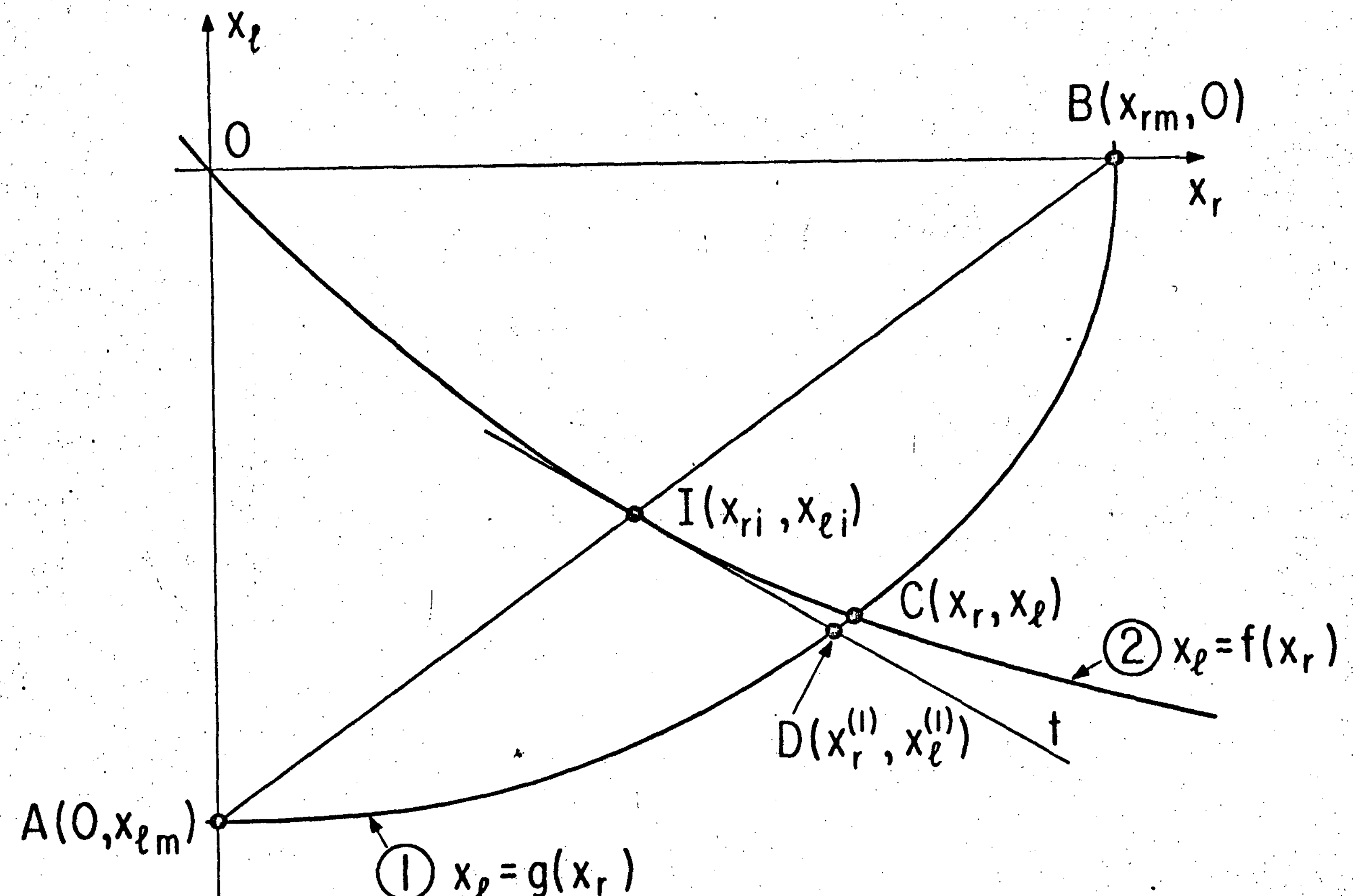
x_ℓ
O
$B(x_{rm}, 0)$
x_r
$I(x_{ri}, x_{\ell i})$
$C(x_r, x_\ell)$
2 $x_\ell = f(x_r)$
$D(x_r^{(1)}, x_\ell^{(1)})$
t
$A(0, x_{\ell m})$
1 $x_\ell = g(x_r)$

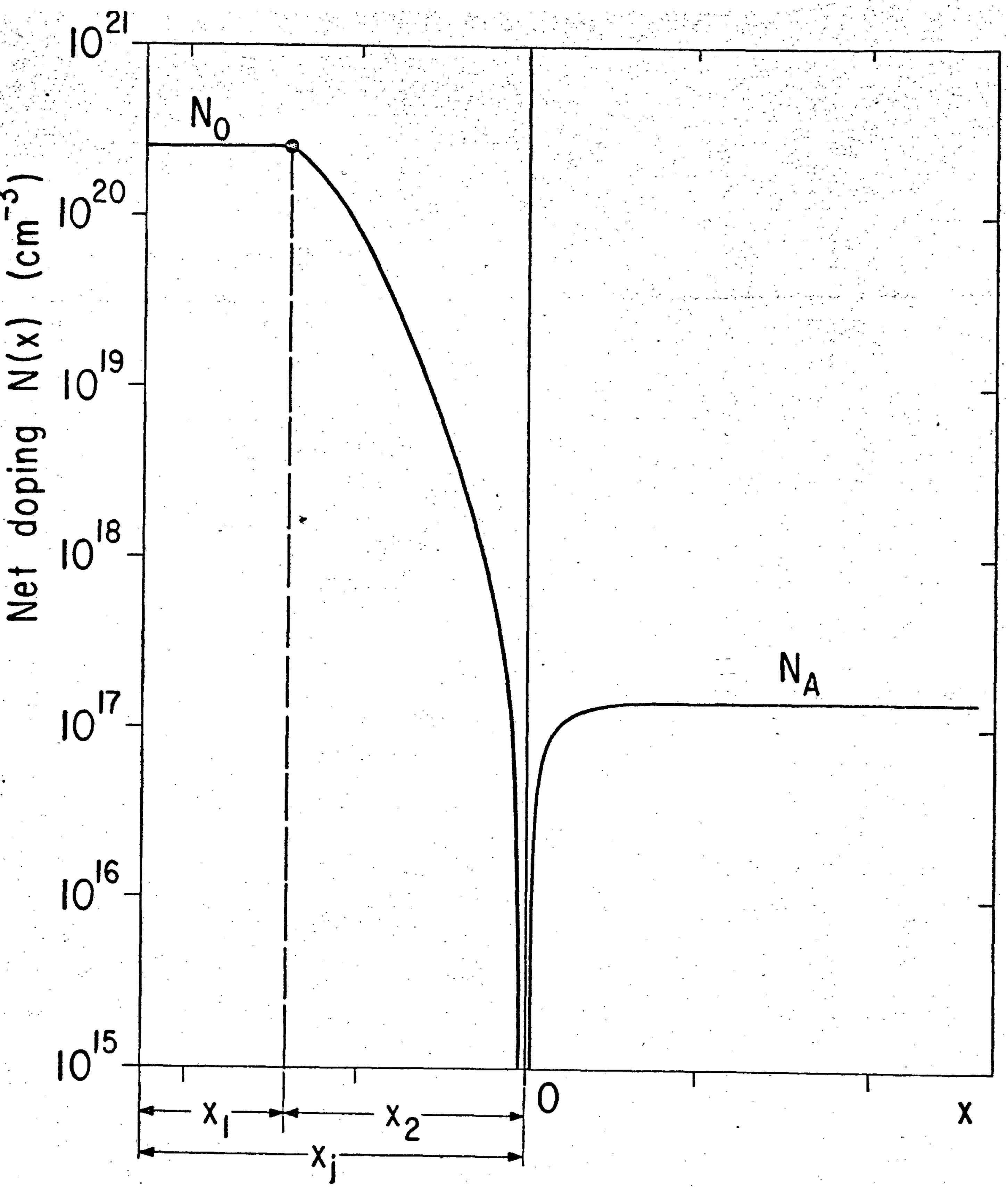
Net doping N(x) (cm^-3)
10^21
10^20
10^19
10^18
10^17
10^16
10^15
N_0
N_A
0
x
x_1
x_2
x_j

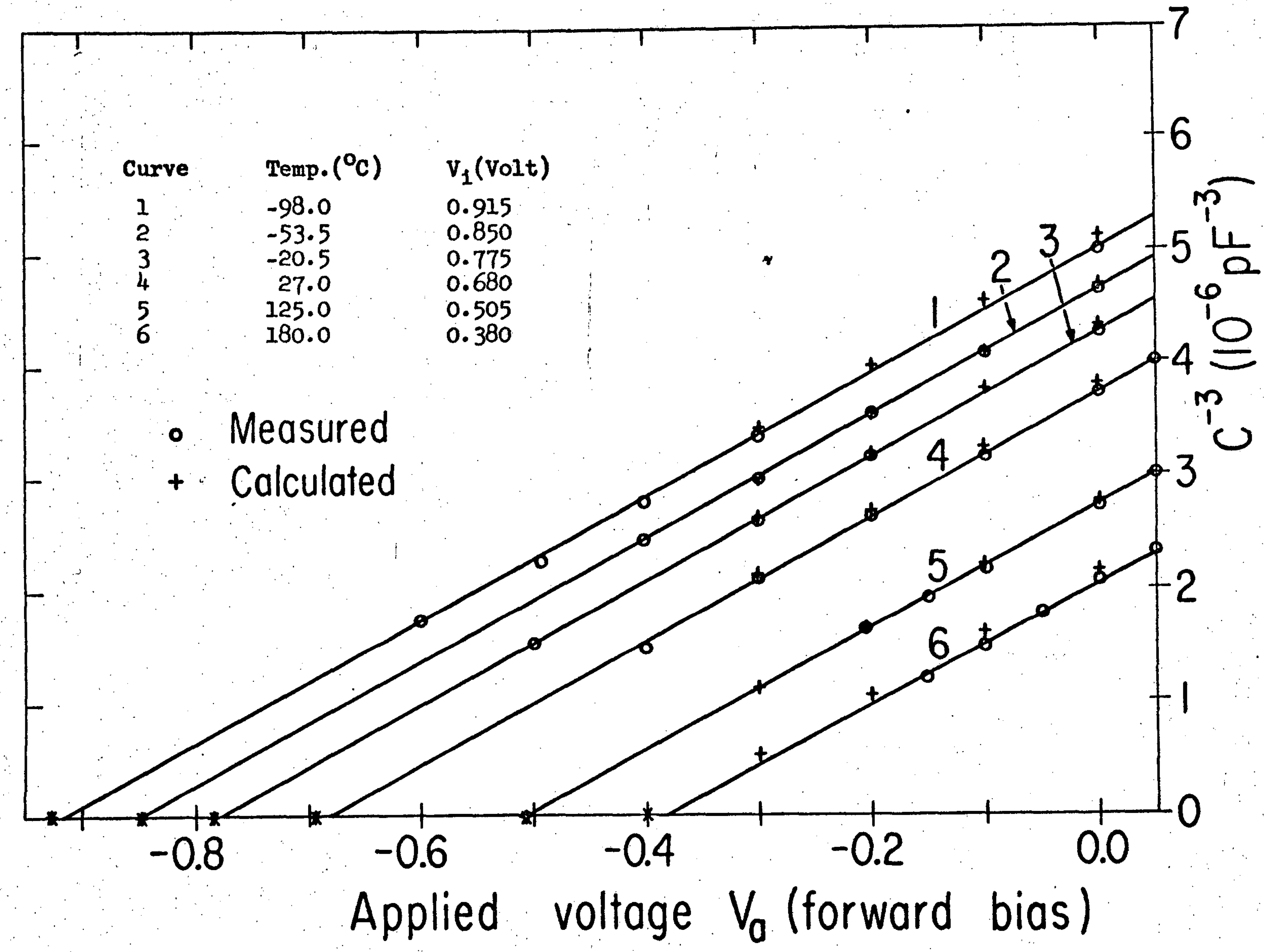

Curve Temp.(°C) V1(Volt)
1 -98.0 0.915
2 -53.5 0.850
3 -20.5 0.775
4 27.0 0.680
5 125.0 0.505
6 180.0 0.380
o Measured
+ Calculated
1
2
3
4
5
6
7
6
5
4
3
2
1
0
C-3 (10-6 pF-3)
-0.8
-0.6
-0.4
-0.2
0.0
Applied voltage Va (forward bias)

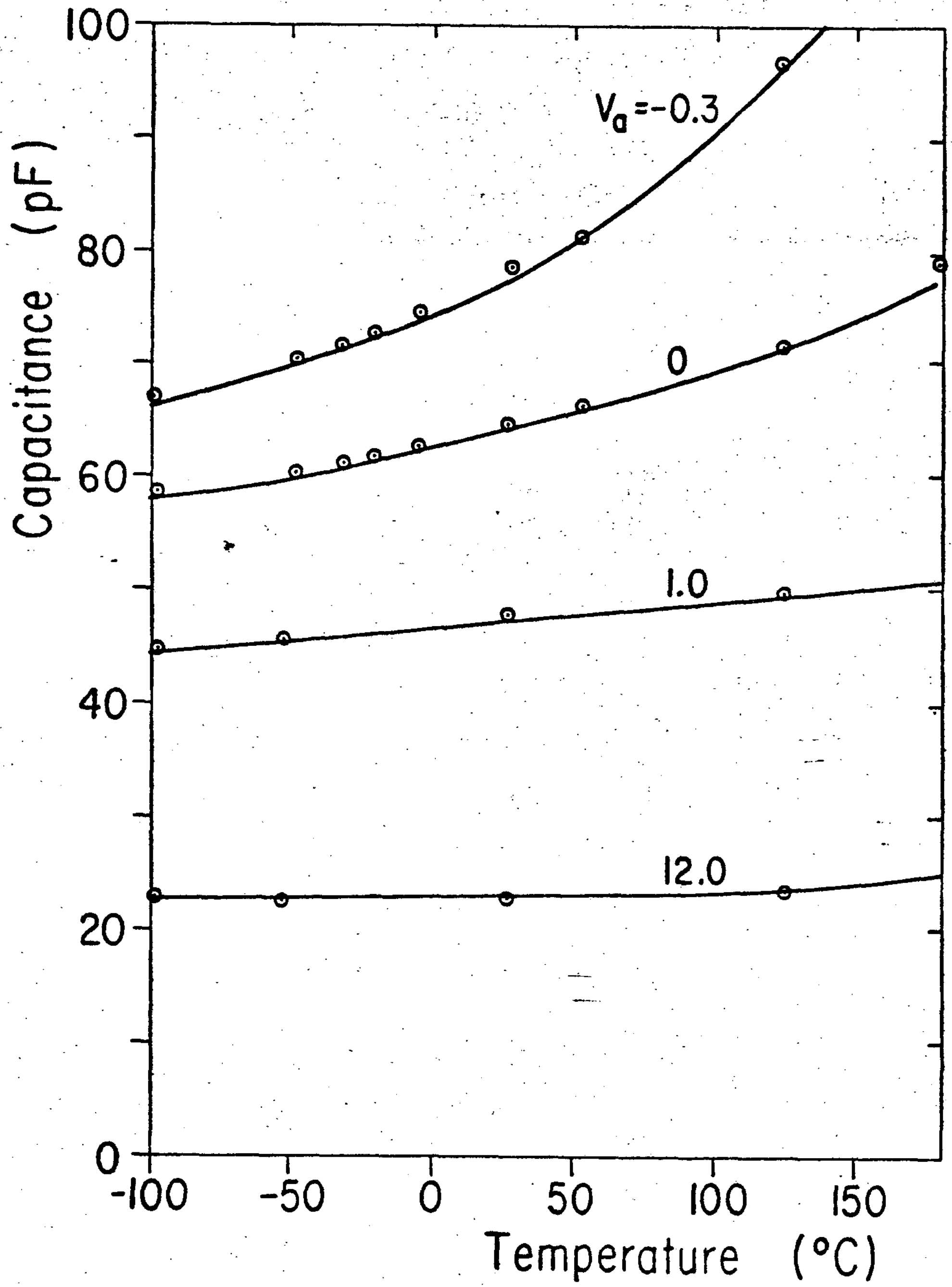

100
80
60
40
20
0
-100
-50
0
50
100
150
Capacitance (pF)
Temperature (°C)
$V_a = -0.3$
0
1.0
12.0

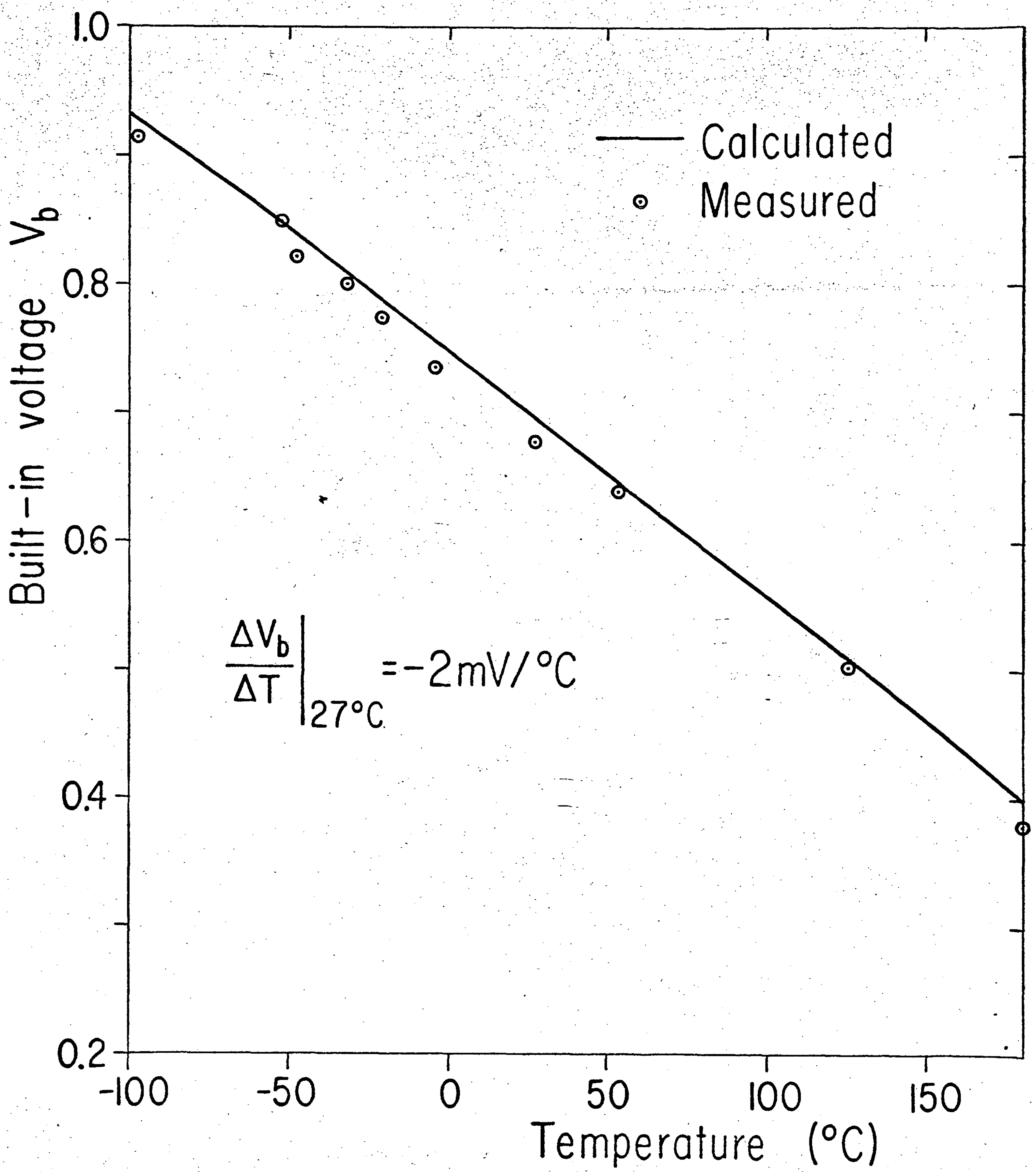

Calculated
Measured
Built-in voltage V_b
Temperature (°C)
$\left.\frac{\Delta V_b}{\Delta T}\right|_{27°C} = -2 mV/°C$
1.0
0.8
0.6
0.4
0.2
-100
-50
0
50
100
150

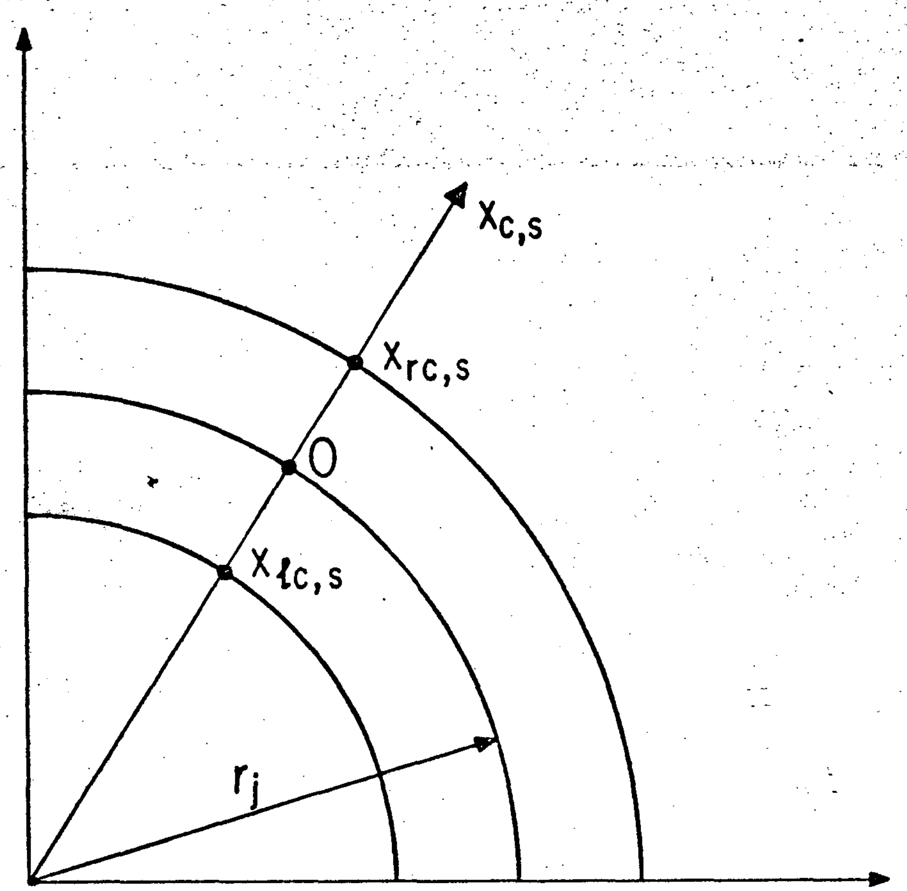

$x_{c,s}$
$x_{rc,s}$
O
$x_{\ell c,s}$
r_j